Dynamic Modeling and Simulation of a Three-wheeled Electric Car

Goran Vasiljevic*, Zoran Vrhovski†, Stjepan Bogdan *
*Faculty of Electrical Engineering and Computing
University of Zagreb
Unska 3, 10000 Zagreb, CROATIA
†Bjelovar Technical College
Trg Eugena Kvaternika 4, 43000 Bjelovar, CROATIA

***Abstract*—We present a non-linear model of a small three wheeled electric car with one rear wheel and two front steered wheels. Each wheel is actuated by a permanent magnet synchronous in-wheel motor. The model was created for development and testing of advanced control algorithms for increasing the car's performance and safety. It includes models of electric motor, non-linear tire-road characteristics, longitudinal and lateral dynamics, a realistic suspension system and the option to influence car's weight and its distribution.**

Index terms - electric car, three wheel, in-wheel motor, modeling.

I. Introduction

The development of electric vehicles has been exponential in recent years due to the high oil prices on world market, as well as the development of longer-lasting batteries and stronger and more efficient electric motors. Electric vehicles have several advantages compared to vehicles with an internal combustion engine. Some of them are: no emission of glass-effect gases, better torque characteristics, higher motor efficiency, the possibility of returning energy to batteries and many others. In case of in-wheel motors, the benefits are even greater: each wheel can be controlled independently, making torque vectoring trivial by simply setting a different torque reference to each wheel it is possible to give negative torque to one wheel and positive to another, there is no need for a mechanical differential, etc. Electric vehicles also have certain drawbacks, mainly related to battery size, charging time and capacity.

In cities, with an ever-growing concentration of vehicles, air and noise pollution present a permanent problem. Small electric car produces no gases and a limited amount of noise, which makes them ideal for city centers. Small size makes finding a parking space and maneuvering in tight spaces much easier. Since most of people working in a city center, live near that city, range of batteries can in most cases be limited and owners can just recharge them over night.

Three wheeled vehicles have been produced as long as those with four wheels. Three wheels is minimal number to have static stability of a vehicle, while the cost of production and maintance are reduced, especially for all-wheel-drives. A drawback of three-wheeled vehicles is reduced stability, when compared to four-wheel vehicles, especially during cornering.

Work described in this paper is part of an effort to develop a small three-wheeled electric car for city traffic, with in-wheel electric motors. A car has one rear wheel and two steered front wheels. It has been decided to develop a realistic, highly detailed mathematical model and implement it as a simulator capable of producing realistic results needed for the development of several car systems like electronic differential including traction control system, electronic stability system, anti-lock braking system and others. Since small light weight three wheeled car is being modelled, the possibility of adding extra weight to the car is included, which effects position of center of gravity (COG) and car's moments of inertia. Nominal values of car's parameters apply for the empty vehicle, so extra weight can be those of passengers in the car or extra load transported by the car. Force sensors can detect changes in vehicle's weight and its distribution and compensate for stability algorithms.

The paper is organized in following way. In section II related work is described, including an overview of existing simulators. Section III gives an overview of the full car model. In section IV some simulation results are presented and in section V a short conclusion is givven.

II. Related work

There have been many vehicle models of different detail and complexity, most of whom are designed for four wheeled vehicles. There are many works describing only certain aspect of vehicles. Detailed description of tire-ground friction is given in [2]. Lateral and longitudinal car dynamics modeling can be found in [3] (control of yaw dynamics), [4](bounding lateral motion for lane keeping), [5] (control of front-wheel steering and breaking forces) and many others. Detailed suspension description and modeling of four wheeled vehicles used for active suspension control is given in [6–9]. Authors in [10–17] present in detail all aspects of ground vehicles including tire characteristics, longitudinal and lateral dynamics, suspension dynamics and aerodynamics.

Work on three wheeled vehicle modeling was not as extensive as for those with four wheels. Authors in [18] gives a comparison between different configurations of three wheeled vehicles and their stability analysis compared to four wheeled vehicles. The modeling procedure and safety analysis for a

three-wheeled Indian rickshaw auto with one forward and two rear wheels are given in [19, 20]. Authors in [21–23] describes three wheeled tilting vehicles. Design of three wheeled vehicles for solar power racing cars is described in [24].

There is a number of commercial and non-commercial car simulators of different levels of detail and complexity, created using different tools. Authors in [25] present simulator developed at Texas A&M University for simulating electric and hybrid vehicles. An overview of US Department of Energy ADVISOR simulator developed in Simulink is given in [26]. Authors in [27, 28] describes commercial Vehicle Dynamics library for Modelica simulator. LMS and dSpace presented commercial Simulink simulators capable of real-time simulations. Optimum vehicle dynamics solutions presented realistic simulator with 3D visualization.

Like many of these papers, this paper presetnts full model of the car. Model in this paper differs from others because it presents full model with suspension of electric three-wheeled car with two front steered wheels featuring the ability to add extra and distributed weight to the model.

III. Car model

The car model consists of several interconnected parts:

- Motor system
- Wheel system
- Longitudinal and lateral dynamics
- Roll, pitch and yaw motion
- Suspension system
- Road curvature modeling

Using energy stored in batteries, the motor system embedded in the wheel produces torque, which is transmitted as a force to the ground on tire-ground contact surface. Force acting on the ground produces counter force acting on the wheel. Forces acting on wheels act together on car's COG as linear forces creating longitudinal and lateral motion, as well as rotational forces creating yaw motion and also roll and pitch motions which are limited by the suspension system. Height of the ground under each wheel and roll and pitch motion influence the car's vertical motion.

A. Motor system

There is one in-wheel permanent magnet synchronous motor (PMSM) embedded in every wheel.

According to [1] PMSM is described in rotor reference frames as follows:

$$\begin{aligned} u_d &= R_S i_d + L_s \frac{di_d}{dt} - \omega \Psi_q \\ u_q &= R_S i_q + L_s \frac{di_q}{dt} + \omega \Psi_d \\ \Psi_d &= L_s i_d + \Psi_r \\ \Psi_q &= L_s i_q \\ T &= \frac{3}{2} p(\psi_r i_q + (L_d - L_Q) i_q i_d) \end{aligned} \tag{1}$$

where u_d and u_q are d and q reference axis voltages, i_d and i_q are d and q reference axis currents, Ψ_r represents rotor flux linkages and T is the torque produced by the motor.

According to (1) motor torque can be controlled directly by current i_q if the current i_d is held at zero. Currents i_q and i_d are controlled using standard PI controller. Standard PMSM model is used to model motor in Simulink.

Motor system produces torques for each wheel based on torque references, which are inputs to the model.

Inputs to motor system are rotational speeds and angles of every wheel and torque references. Outputs are torques produced by motors in every wheel.

B. Wheel system

If rolling resistance is ignored, the following equation can be written for a wheel's angular velocity:

$$J_w \cdot \dot{\omega}_w = T_m - T_b - R_w \cdot F_t \tag{2}$$

where J_w is wheel's moment of inertia, ω_w is wheel's angular velocity, T_m is torque generated by the motor, T_b is the torque generated by the brake system, R_w is the radius of the wheel and F_t is the wheel's traction force:

$$\begin{aligned} F_{tfl} &= F_{zfl} \cdot \mu(\lambda_{fl}) \\ F_{tfr} &= F_{zfr} \cdot \mu(\lambda_{fr}) \\ F_{tr} &= F_{zr} \cdot \mu(\lambda_r) \end{aligned} \tag{3}$$

where F_{tfl}, F_{tfr} and F_{tr} are wheels' traction forces of forward left, forward right and rear wheel, F_{zfl}, F_{zfr} and F_{zr} are surface reaction forces of forward left, forward right and rear wheel and $\mu(\lambda)$ is longitudinal friction coefficient dependent on slip coefficient λ.

Side forces acting on each wheel are:

$$\begin{aligned} F_{sfl} &= F_{zfl} \mu(\alpha_{fl}) \\ F_{sfr} &= F_{zfr} \mu(\alpha_{fr}) \\ F_{sr} &= F_{zr} \mu(\alpha_r) \end{aligned} \tag{4}$$

where F_{sfl}, F_{sfr} and F_{sr} are side forces acting on forward left, forward right and rear wheel and $\mu(\alpha)$ is the side friction coefficient dependent on sideslip angle α (Fig. 1). Slip coefficient λ is calculated using the following equation [10]:

$$\lambda = \frac{R_w \omega_w - v}{max(\omega_w, v)} \tag{5}$$

where v is longitudinal velocity of the wheel calculated for each wheel using following equations:

$$\begin{aligned} v_{fl} &= (v_x - \frac{T_f}{2}\dot{\psi}) \cos\delta_{fl} + (v_y + a\dot{\psi}) \sin\delta_{fl} \\ v_{fr} &= (v_x + \frac{T_f}{2}\dot{\psi}) \cos\delta_{fr} + (v_y + a\dot{\psi}) \sin\delta_{fr} \\ v_r &= v_x + \Delta y_{cg}\dot{\psi} \end{aligned} \tag{6}$$

where T_f is front axle length, a is the distance from car's center of gravity to the front axle, Δy_{cg} is the shift along the y axis from rear wheel to center of gravity (explained in detail later) , v_x and v_y are vehicle's longitudinal and lateral velocity, respectively, ψ is vehicle's yaw angle, δ_{fl} and δ_{fr} are steering

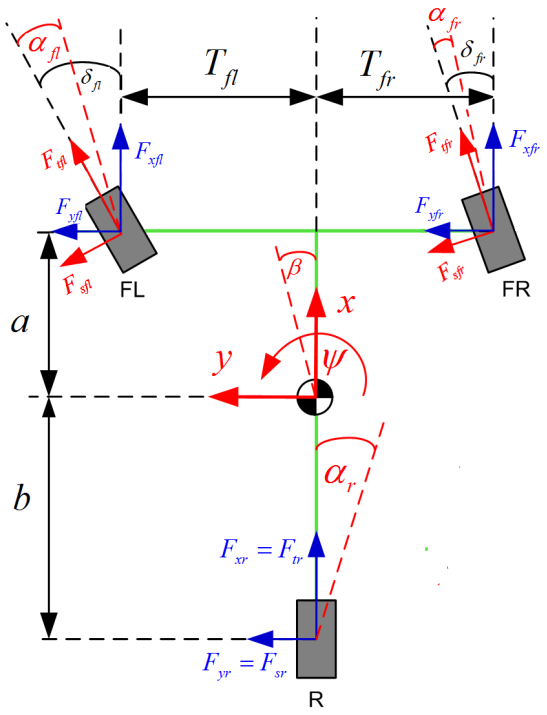

Fig. 1. Forces acting on car

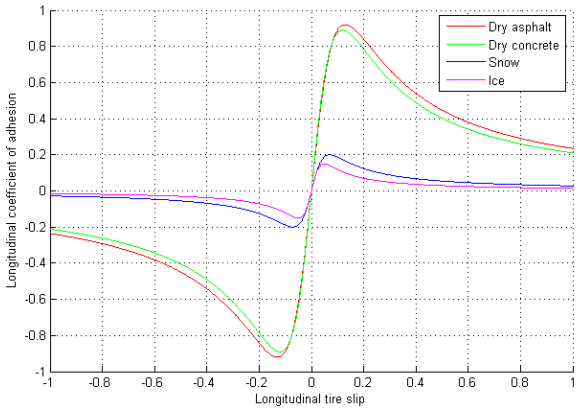

Fig. 2. $\mu - \lambda$ curve for different road conditions

angles of left and right front wheels (Fig. 1). These quantities are interdependent according to Ackerman condition [10]:

$$\frac{1}{\tan\delta_{fr}} - \frac{1}{\tan\delta_{fl}} = \frac{T_{fl} + T_{fr}}{a + b} \tag{7}$$

Steering angles δ_{fl} and δ_{fr} are dependent on the car's steering angle (defined by turning of the steering wheel) which is an input signal to the model.

Friction coefficient $\mu(\lambda)$ can be approximated by the function [29]:

$$\mu(\lambda) = \frac{2\lambda_p \mu_p}{\lambda_p^2 + \lambda^2}\lambda \tag{8}$$

where μ_p and λ_p are peak values of $\mu - \lambda$ curve (shown in Fig. 2).

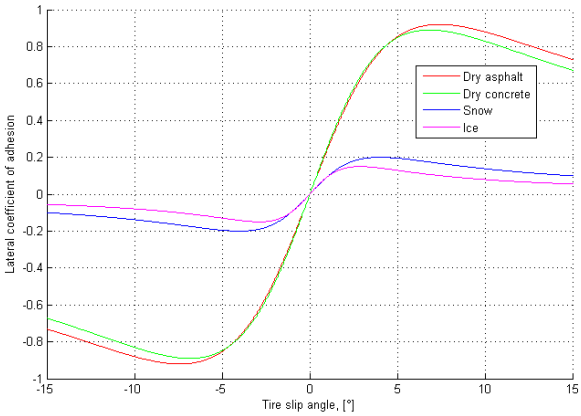

Fig. 3. $\mu - \alpha$ curve for different road conditions

Sideslip angle α is determined using following equations:

$$\begin{aligned}
\alpha_{fl} &= \delta_{fl} - \arctan\left(\frac{v_y + a\dot{\psi}}{v_x - \frac{T_f}{2}\dot{\psi}}\right) \\
\alpha_{fr} &= \delta_{fr} - \arctan\left(\frac{v_y + a\dot{\psi}}{v_x + \frac{T_f}{2}\dot{\psi}}\right) \\
\alpha_{fl} &= 0 + \arctan\left(\frac{b\dot{\psi} - v_y}{v_x + \Delta y_{cg}\dot{\psi}}\right)
\end{aligned} \tag{9}$$

where b is the distance from car's center of gravity to the rear axle.

Friction coefficient $\mu(\alpha)$ can be approximated by the function:

$$\mu(\alpha) = \frac{2\alpha_p \mu_p}{\alpha_p^2 + \alpha^2}\alpha \tag{10}$$

where μ_p and α_p are peak values of $\mu - \alpha$ curve (shown in Fig. 3).

Parameters μ_p, λ_p and α_p define functions which approximates friction between wheel and ground. Fig. 2 and 3 shows typical friction characteristics between wheel and dry asphalt, dry concrete, snow and ice.

Inputs to the wheel system are torques produced by each motor, torques produced by the brake system, longitudinal and lateral velocity of center of gravity, yaw rate, steering angles and surface reaction forces. Outputs are rotational speeds, traction and side forces of every wheel

C. Longitudinal and lateral dynamics

Forces acting in x and y direction (Fig. 1) at each wheel are:

$$\begin{aligned}
F_{xfl} &= F_{tfl}\cos\delta_{fl} - F_{sfl}\sin\delta_{fl} \\
F_{yfl} &= F_{tfl}\sin\delta_{fl} + F_{sfl}\cos\delta_{fl} \\
F_{xfr} &= F_{tfr}\cos\delta_{fr} - F_{sfr}\sin\delta_{fr} \\
F_{yfr} &= F_{tfr}\sin\delta_{fr} + F_{sfr}\cos\delta_{fr} \\
F_{xr} &= F_{tr} \\
F_{yr} &= F_{sr}
\end{aligned} \tag{11}$$

where F_{xfl}, F_{yfl}, F_{xfr}, F_{yfr}, F_{xr} and F_{yr} are forces acting along x and y direction at forward left, forward right, and rear wheel.

Longitudinal forces acting on car's center of gravity are [10]:

$$m_t(\dot{v_x} - v_y\dot{\psi}) = F_{xfl} + F_{xfr} + F_{xr} - F_{ad\_x} - F_g \quad (12)$$

where m_t is vehicle mass, F_{a_dx} is aerodynamic drag in x direction and F_g is gravitational force:

$$F_g = m \cdot g \cdot \sin\gamma \quad (13)$$

where γ is road slope angle.

F_{ad_x} is calculated using following formula:

$$F_{ad\_x} = \frac{1}{2}\rho C_{ad} A_F v_x^2 sgn(v_x) \quad (14)$$

where ρ is the mass density of the air, C_d is air drag coefficient and A_F is frontal area of the car.

Lateral forces acting on car's center of gravity are [10]:

$$m_t(\dot{v_y} - v_x\dot{\psi}) = F_{yfl} + F_{yfr} + F_{yr} \quad (15)$$

Velocities v_x and v_y which define longitudinal and lateral dynamics are calculated using equations (12) and (15).

Inputs to longitudinal and lateral dynamics system are traction and side forces of every wheel, yaw rate, steering angles and slope. Outputs are longitudinal and lateral speed, longitudinal and lateral forces acting on each wheel and aerodynamics drag.

D. Roll, pitch and yaw motion

Car's roll, pitch and yaw motion are calculated with respect to the center of gravity.

Considering vehicles small size and weight, it has been decided to model the influence of additional weight (driver) on the vehicle's dynamics. Fig. 4 shows how the driver's weight influences the center of gravity.

With respect to the coordinate system in back right corner of the car it can be written (blue on Fig. 4):

$$X_{cg\_new} = \frac{X_{cg\_old} m_{t\_old} + X_d m_d}{m_t} \quad (16)$$

where m_{t_old} is the mass of empty vehicle, m_d is the mass of the driver, X_{cg_new} is x coordinate of the new center of gravity X_{cg_old} is x coordinate of the old center of gravity and X_d is x coordinate of the driver.

Equation (16) gives following:

$$\begin{aligned}(X_{cg\_new} - X_{cg\_old})\, m_t &= (X_d - X_{cg\_old})\, m_d \\ \Rightarrow \Delta x_{cg} &= \frac{m_d}{m_t}\Delta x_d\end{aligned} \quad (17)$$

where Δx is shift of center of gravity along x axis and Δx_d is x coordinate of the driver in the coordinate system of old center of gravity.

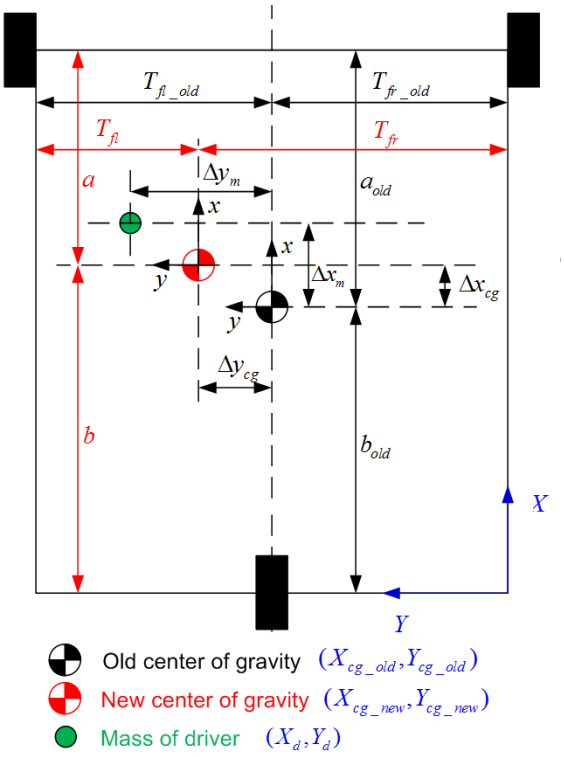

Fig. 4. Influence of driver's weight to COG

Similar to (17) it is possible to get shift of the center of gravity along y and z axes:

$$\begin{aligned}\Delta y_{cg} &= \frac{m_d}{m_t}\Delta y_d \\ \Delta z_{cg} &= \frac{m_d}{m_t}\Delta z_d\end{aligned} \quad (18)$$

where Δy_{cg} and Δz_{cg} are shifts of the center of gravity along y and z axes.

Position of the center of gravity affects some parameters of the car (Fig. 4) used in car's dynamics equations:

$$\begin{aligned}a &= a_{old} - \Delta x_{cg} \\ b &= b_{old} + \Delta x_{cg} \\ T_{fl} &= T_{fl\_old} - \Delta y_{cg} \\ T_{fr} &= T_{fr\_old} + \Delta y_{cg} \\ h_{cg} &= h_{cg\_old} - \Delta h_{cg}\end{aligned} \quad (19)$$

where a is the distance to the front axle, b is the distance to the rear axle, T_{fl} is the distance to the left wheel along the y axis, and T_{fr} is the distance to the right wheel along the y axis all with respect to the COG.

Under the assumption that the car's shape can be approximated by a rectangular box (Fig. 5) and that it has constant density, new moments of inertia I_{xx}, I_{yy} and I_{zz} can be

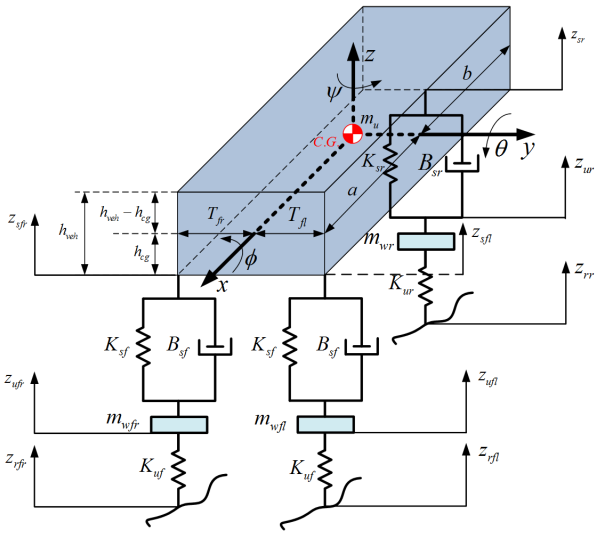

Fig. 5. Suspension

calculated according to:

$$\begin{aligned}
\mathrm{I}_{xx} &= \rho \int_{-b}^{a} \int_{-\mathrm{T_{fr}}}^{\mathrm{T}_{fl}} \int_{-\mathrm{h_{cg}}}^{\mathrm{h_{veh}}-\mathrm{h_{cg}}} \left(y^2+z^2\right) dxdydz = \\
&= \frac{m_t}{3}\left(3{\mathrm{h_{cg}}}^2 - 3\mathrm{h_{cg}h_{veh}} + {\mathrm{h_{veh}}}^2 + {\mathrm{T_{fl}}}^2 - \mathrm{T_{fl}T_{fr}} + {\mathrm{T_{fr}}}^2\right) \\
\mathrm{I}_{yy} &= \rho \int_{-b}^{a} \int_{-\mathrm{T_{fr}}}^{\mathrm{T}_{fl}} \int_{-\mathrm{h_{cg}}}^{\mathrm{h_{veh}}-\mathrm{h_{cg}}} \left(x^2+z^2\right) dxdydz = \\
&= \frac{1}{3} m_t \left(3{\mathrm{h_{cg}}}^2 - 3\mathrm{h_{cg}h_{veh}} + {\mathrm{h_{veh}}}^2 + a^2 - ab + b^2\right) \\
\mathrm{I}_{zz} &= \rho \int_{-b}^{a} \int_{-\mathrm{T_{fr}}}^{\mathrm{T}_{fl}} \int_{-\mathrm{h_{cg}}}^{\mathrm{h_{veh}}-\mathrm{h_{cg}}} \left(x^2+y^2\right) dxdydz = \\
&= \frac{1}{3} m_t \left(a^2 - ab + b^2 + {\mathrm{T_{fl}}}^2 - \mathrm{T_{fl}T_{fr}} + {\mathrm{T_{fr}}}^2\right)
\end{aligned} \tag{20}$$

where h_{veh} is the height of the vehicle.

Fig. 5 shows the car suspension system with roll, pitch and yaw angles of the sprung mass.

Yaw motion is described using the torque equation with respect to the car's z-axis:

$$\begin{aligned}
I_{zz}\ddot{\psi} = a(F_{yfl}+F_{yfr}) - bF_{yr} - T_{fl}F_{xfl} + \\
+T_{fr}F_{xfr} + \Delta y_{cg}F_{xr}
\end{aligned} \tag{21}$$

where ψ is the yaw angle.

Torque equation with respect to the y-axis gives pitch motion:

$$\begin{aligned}
&I_{yy}\ddot{\theta} = (2aK_{sf} - bK_{sr})z + (2aB_{sf} - bB_{sr})\dot{z} - \\
&-(2a^2K_{sf} + b^2K_{sr})\theta - (2a^2B_{sf} + b^2B_{sr})\dot{\theta} - \\
&-aK_{sf}(z_{ufl} + z_{ufr}) - aB_{sf}(\dot{z}_{ufl} + \dot{z}_{ufr}) + \\
&+bK_{sr}z_{ur} + bB_{sr}\dot{z}_{ur} - F_{ad_x}(h_{ad} - h_{cg}) - \\
&-h_{cg}F_{xfl} - h_{cg}F_{xfr} - h_{cg}F_{xr}
\end{aligned} \tag{22}$$

where θ is the pitch angle, K_{sf} and B_{sf} are forward spring and dampening suspension coefficients, K_{sr} and B_{sr} are rear spring and dampening suspension coefficients, z_{ufl}, z_{ufr} and z_{ur} are forward left, forward right and rear wheel heights, z is the height of sprung mass and h_{ad} is the height from the ground at which aerodynamic drag acts on the car.

Roll motion can be determined by the torque equation with respect to the x-axis:

$$\begin{aligned}
&I_{xx}\ddot{\phi} = -\left(\left({T_{fl}}^2 + {T_{fr}}^2\right)K_{sf} + {\Delta y_{cg}}^2 K_{sr}\right)\phi - \\
&-\left(\left({T_{fl}}^2 + {T_{fr}}^2\right)B_{sf} + {\Delta y_{cg}}^2 B_{sr}\right)\dot{\phi} + \\
&+T_{fl}K_{sf}z_{ufl} + T_{fl}B_{sf}\dot{z}_{ufl} - T_{fr}K_{sf}z_{ufr} - \\
&-T_{fr}B_{sf}\dot{z}_{ufr} - \Delta y_{cg}K_{sr}z_{ur} - \Delta y_{cg}B_{sr}\dot{z}_{ur} + \\
&+h_{cg}F_{yfl} + h_{cg}F_{yfr} + h_{cg}F_{yr}
\end{aligned} \tag{23}$$

where ϕ is roll angle

Inputs to roll, pitch and yaw motion system are longitudinal and lateral forces acting at each wheel, aerodynamics drag, height of COG, vertical speed of COG, heights of each wheel, and vertiacl speeds of each wheel. Outputs are roll angle, roll rate, pitch ange, pitch rate, yaw angle and yaw rate.

E. Suspension

The force equation in z direction acting on car's COG is used to calculate height of sprung mass (Fig. 5):

$$\begin{aligned}
&m_s\ddot{z} = -m_s g cos(\gamma) - (2K_{sf} + K_{sr})z - \\
&-(2B_{sf} + B_{sr})\dot{z} + (2aK_{sf} - bK_{sr})\theta + \\
&+(2aB_{sf} - bB_{sr})\dot{\theta} + (2\Delta y_{cg}K_{sf} + \Delta y_{cg}K_{sr})\phi + \\
&+(2\Delta y_{cg}B_{sf} + \Delta y_{cg}B_{sr})\dot{\phi} + K_{sf}(z_{ufl} + z_{ufr}) + \\
&+B_{sf}(\dot{z}_{ufl} + \dot{z}_{ufr}) + K_{sr}z_{ur} + B_{sr}\dot{z}_{ur}
\end{aligned} \tag{24}$$

where m_s is the sprung mass.

Heights of each wheel z_{ufl}, z_{ufr} and z_{ur} are determined using force equations in z direction in the position of each wheel:

$$\begin{aligned}
&m_{wfl}\ddot{z}_{ufl} = -m_{wfl}g + K_{sf}z_{sfl} + B_{sf}\dot{z}_{sfl} - \\
&-K_{sf}z_{ufl} - B_{sf}\dot{z}_{ufl} + K_{uf}(z_{rfl} - z_{ufl}) \\
&m_{wfr}\ddot{z}_{ufr} = -m_{wfr}g + K_{sf}z_{sfr} + B_{sf}\dot{z}_{sfr} - \\
&-K_{sf}z_{ufr} - B_{sf}\dot{z}_{ufr} + K_{uf}(z_{rfr} - z_{ufr}) \\
&m_{wr}\ddot{z}_{ur} = -m_{wr}g + K_{sr}z_{sr} + B_{sr}\dot{z}_{sr} - \\
&-K_{sr}z_{ur} - B_{sr}\dot{z}_{ur} + K_{ur}(z_{rr} - z_{ur})
\end{aligned} \tag{25}$$

where z_{rfl}, z_{rfr} and z_{rr} are road heights under each wheel, m_{wfl}, m_{wfr} and m_{wr} are masses of forward left, forward right and rear wheel, and where:

$$\begin{aligned}
z_{sfl} &= z - a\theta + T_{fl}\phi \\
z_{sfr} &= z - a\theta - T_{fr}\phi \\
z_{sr} &= z + b\theta - \Delta y_{cg}\phi
\end{aligned} \tag{26}$$

In (25), $K_{uf}(z_{rfl}-z_{ufl})$, $K_{uf}(z_{rfr}-z_{ufr})$, $K_{ur}(z_{rr}-z_{ur})$ are vertical forces of each wheel acting at the surface:

$$\begin{aligned}
F_{zfl} &= K_{uf}(z_{rfl} - z_{ufl}) \\
F_{zfr} &= K_{uf}(z_{rfr} - z_{ufr}) \\
F_{zr} &= K_{ur}(z_{rr} - z_{ur})
\end{aligned} \tag{27}$$

When the wheel is in contact with the ground, forces F_{zfl}, F_{zfr} and F_{zr} are positive, but when the wheel is in the air, according to (27), forces are negative and act on the wheel towards the ground. This scenario is physically impossible, so it is necessary to set the lower limit of the forces in (27) to zero.

Inputs to suspension systems are roll angle, roll rate, pitch angle, pitch rate, height of ground under each wheel, and road slope. Outputs are height of COG, vertical speed of COG, height of each wheel, vertical speed of each wheel and surface reaction forces of each wheel.

F. Road curvature modeling

The following equations describe the car's global position in the horizontal plane:

$$\begin{aligned} \dot{X_E} &= v_x \cos\psi - v_y \sin\psi \\ \dot{Y_E} &= v_x \sin\psi - v_y \cos\psi \end{aligned} \tag{28}$$

where X_E and Y_E are coordinates of car's COG in the global coordinate system.

If 3D road curvature is described by the equation:

$$z = f(x, y) \tag{29}$$

it is necessary to find the exact position of each wheel in the horizontal plane, x_{fl}, y_{fl}, x_{fr}, y_{fr}, x_r and y_r, to calculate and forward values z_{rfl}, z_{rfr} and z_r to the suspension system:

$$\begin{aligned} x_{fl} &= X_E + h_{cg}\sin\theta\cos\psi + h_{cg}\sin\phi\sin\psi + \\ &\quad + a\cos\theta\cos\psi - T_{fl}\cos\phi\sin\psi \\ y_{fl} &= Y_E + h_{cg}\sin\theta\sin\psi + h_{cg}\sin\phi\cos\psi + \\ &\quad + a\cos\theta\sin\psi - T_{fl}\cos\phi\cos\psi \\ x_{fr} &= X_E + h_{cg}\sin\theta\cos\psi + h_{cg}\sin\phi\sin\psi + \\ &\quad + a\cos\theta\cos\psi + T_{fr}\cos\phi\sin\psi \\ y_{fr} &= Y_E + h_{cg}\sin\theta\sin\psi + h_{cg}\sin\phi\cos\psi + \\ &\quad + a\cos\theta\sin\psi + T_{fr}\cos\phi\cos\psi \\ x_r &= X_E + h_{cg}\sin\theta\cos\psi + h_{cg}\sin\phi\sin\psi - \\ &\quad - b\cos\theta\cos\psi - \Delta y_{cg}\cos\phi\sin\psi \\ y_r &= Y_E + h_{cg}\sin\theta\sin\psi + h_{cg}\sin\phi\cos\psi - \\ &\quad - b\cos\theta\sin\psi - \Delta y_{cg}\cos\phi\cos\psi \end{aligned} \tag{30}$$

Ground curvature acting on each wheel is calculated using equations:

$$\begin{aligned} z_{rfl} &= f(x_{fl}, y_{fl}) \\ z_{rfr} &= f(x_{fr}, y_{fr}) \\ z_{rr} &= f(x_r, y_r) \end{aligned} \tag{31}$$

The entire Simulink model is shown in Fig. 6.

IV. Simulation Results

The vehicle model has been tested under various driving conditions. Several results are presented in this section.

Fig. 7 shows yaw rate and path in global coordinates of the car if step torque reference is set to all three wheels and forward left wheel turned by angle 0.3 rad and forward right wheel turned by 0.253 rad (different because of Ackerman condition (7)). Simulation was run twice, with parameters for dry asphalt and with parameters for ice. Results show that on ice, at certain velocity the car begins to understeer because the lateral force is too small to keep the car cornering at the desired rate.

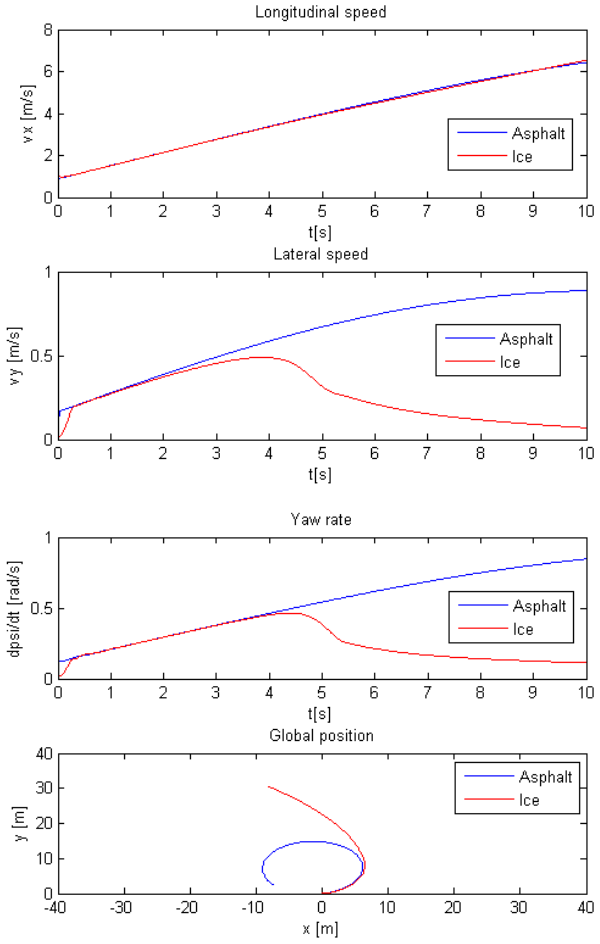

Fig. 7. Cornering on asphalt and ice

Fig. 8 shows the car's path in global coordinates if step torque reference is set to all three wheels, for the case of an empty car, and for the case of a driver weighting 70kg, positioned 40cm to the right and 10cm forward with respect to the COG. Extra weight moves the COG from the center, which influences yaw motion of the car in parts $\Delta y_{cg} F_{xr}$ and $-T_{fl}F_{xfl} + T_{fr}F_{yfr}$ of equation (21) and the car begins to slowly turn to one side.

Fig. 9 shows longitudinal velocity and pitch angle response if step torque reference is set to all three wheels. Results show that the car accelerates almost linearly (aerodynamic drag is increasing with velocity), and that because of almost constant pitch torque acting on the COG, pitch angle is constant after an initial transition period.

Current research, based on described model, is devoted to design of electronic differential based on torque vectoring and

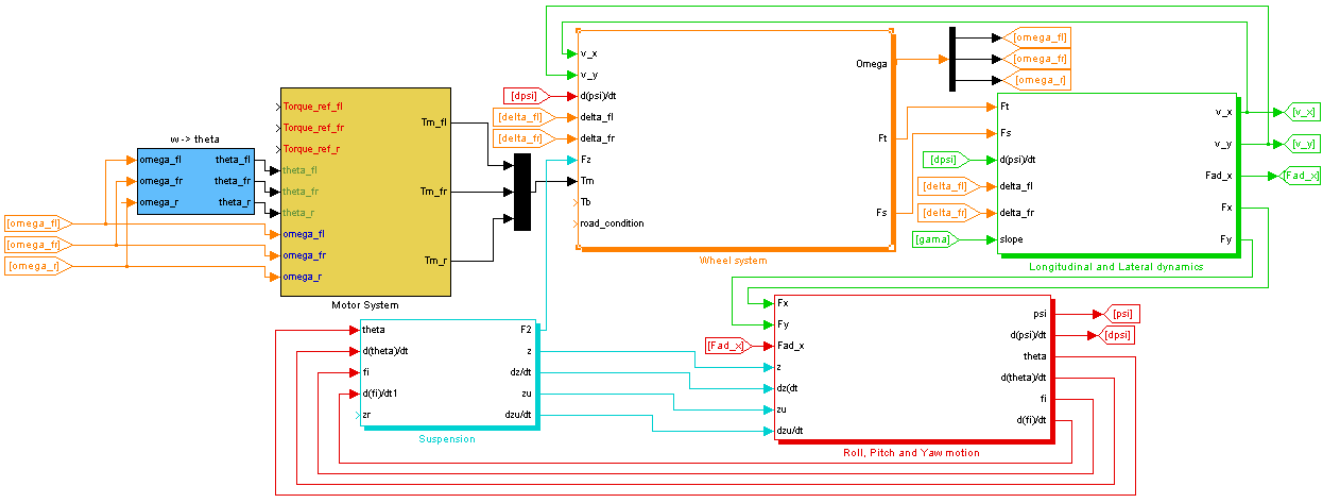

Fig. 6. Simulink model of three wheeled electric car

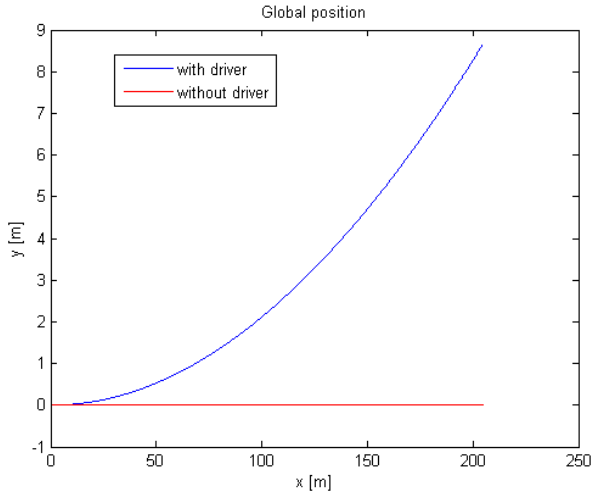

Fig. 8. Response with and without driver's mass

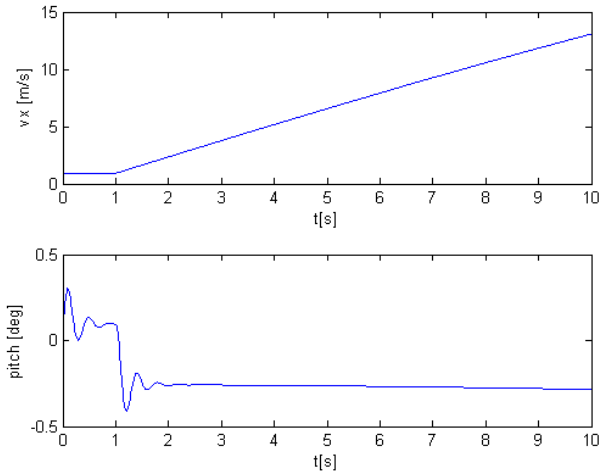

Fig. 9. Accelerating car

its implementation on a real car (Fig. 10). Fig. 11 shows car's path when cornering on the ice with and without electronic differential comprising torque vectoring. When car begins to understeer control algorithm reduces torque in such way that yaw rate returns to normal.

V. Conclusion

In this paper a detailed mathematical model and a Simulik-based simulator of a small, three-wheeled electric car is presented. Simulation results have confirmed that the modeled vehicle behaves in a physically intuitive way under various simulated conditions. Thus, the presented model can be the basis for the development of electronic differential and belonging subsystems like traction control system, electronic stability control system and others. A further useful feature is the ability to add extra weight to the model, to account for the influence of the driver, passengers and cargo on vehicle dynamics. Vehicle's weight and its distribution can be detected by force sensors and can be used for adaptation of the stability control algorithms.

VI. Acknowledgment

The work described in this paper has been performed within the project "Electronic differential for small electric city car" supported by the grant from the Croatian Science Foundation (HRZZ), Republic of Croatia.

References

[1] R. Krishnan, *Electric Motor Drives: Modeling, Analysis and Control*, Prentice Hall inc. Upeer Saddle River, New Jersey, 2001.

[2] H. B. Pacejka *Tyre and Vehicle Dynamics*, SAE Inernational and Elsevier, 2005.

Fig. 10. Experimental three-wheeled car

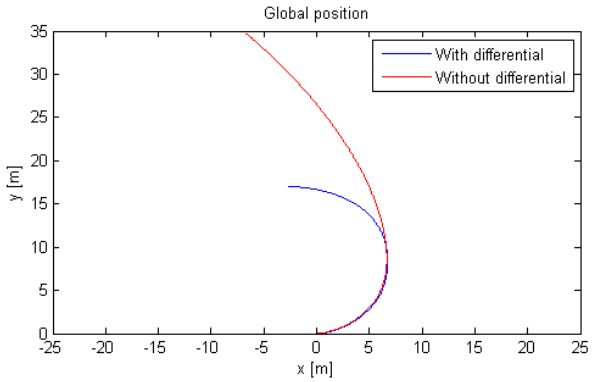

Fig. 11. Cornering on ice with and without differential

[3] S. Anwar *Generalized predictive control of yaw dynamics of a hybrid brake-by-wire equipped vehicle*, Mechatronics, Volume 15, Issue 9, 2005.

[4] E. J. Rossetter, J. C. Gerdes *Performance guarantees for hazard based lateral vehicle control*, ASME Conference Proceedings 2002

[5] M. J. L. Boada, B. L. Boada, A. Muñoz, V. Díaz *Integrated control of front-wheel steering and front braking forces on the basis of fuzzy logic*, Journal of Automobile Engineering, vol. 220, no. 3, 2006.

[6] Jaehoon Lee, Jonghyun Lee, S. Heo *Full Vehicle Dynamic Modeling for Chassis Controls*, FISITA, 2008

[7] S. Ikenaga, F. L. Lewis, J. Campos, L. Davis *Active Suspension Control of Ground Vehicle based on a Full-Vehicle Model*, American Control Conference 2000.

[8] J. Huang, J. Ahme, A. Kojic, J. Hathout *Control Oriented Modeling for Enhanced Yaw Stability and Vehicle Steerability*, American Control Conference 2004.

[9] J. Campos, L. Davis, F. L. Lewis, S. Ikenaga, S. Scully, M. Evans *Active Suspension Control of Ground Vehicle Heave and Pitch Motions*, Proceedings of MED99, Israel, 1999.

[10] R. N. Jazar *Vehicle dynamics*, Springer Science+Business Media, LLC, New York, 2008.

[11] J. Y. Wong, *Theory of ground vehicles*, John Wiley & Sons Inc, New York, 2001

[12] K. Popp, W. Schiehlen *Ground vehicle dynamics*, Springer-Verlag Berlin Heidelberg, 2010

[13] W. F. Milliken, D. L. Milliken *Race car vehicle dynamics*, Society of Automotive Engineers, Inc, Warrendale, USA, 1995.

[14] T. D. Gillespie *Fundamentals of Vehicle Dynamics*, Society of Automotive Engineers, Inc, Warrendale, USA, 1992.

[15] R. Rajamani *Vehicle Dynamics and Control*, Springer Science+Business Media Inc., New York, 2006.

[16] M. Blundell, D. Harty *The Multibody Systems Approach to Vehicle Dynamics*, Elsevier Butterworth-Heinmann, Burlington, 2004.

[17] G. Rill *Vehicle dynamics*, Fachhochschule Reensburg, University of applied scinces, Hochschule für technik, Lecture notes, 2006.

[18] J. C. Huston, B. J. Graves, D. B. Johnson *Three Wheeled Vehicle Dynamics*, Society of Automotive Engineers, 820139, 1982.

[19] S. Mukherjee, D. Mohan, T. R. Gawade *Three wheeled scooter taxi: A safety analysis*, Sadhana, Vol 32. Part 4., 2007.

[20] T.R. Gawade, S. Mukherjee, D. Mohan *Six-degree-of-freedom three-Wheeled-vehicle model validation*, Proceedings of the Institution of Mechanical Engineers, Part D: Journal of Automobile Engineering, 2005.

[21] J. Berote, A. van Poelgeest, J. Darling, K. Edge, Andrew Plummer *The dynamics of a three-wheeled narrow-track tilting vehicle*, FISITA, 2008.

[22] J. Gohl, R. Rajamani, L. Alexander, P. Starr *The Development of Tilt-Controlled Narrow Ground Vehicles*, Proceedings of American Control Conference, 2002.

[23] C. R. van der Bring, H. M. Kroonen *DVC - The banking technology driving the CARVER vehicle class*, AVEC 2004.

[24] P. J. Starr *Designing Stable Three Wheeled Vehicle With Application to Solar Powered Racing Cars*, Working paper, University of Minnesota Solar Vehicle Project, 2006.

[25] K. L. Butler, M. Eshani, P. Kamath. *A Matlab-Based Modeling and Simulation Package for Electric and Hybrid Electric Vehicle Design*, IEEE Transactions on Vehicular Technology, vol. 48, no. 6, 1999.

[26] T. Markel, A. Brooker, T. Hendricks, V. Johnson, K. Kelly, B. Kramer, M. O'Keefe, S. Sprik, K. Wipke *ADVISOR: a systems analysis tool for advanced vehicle modeling*, Journal of Power Sources 110, 2002.

[27] J. Andreasson, M. Gafvert *The VehcileDynamics Library - Overview and Applications*, Modelica 2006.

[28] J. Andreasson *The Vehicle Dynamics Library: New Concepts and New Fields of Applications*, Proceedings of 8th Modelica Conference, 2011.

[29] W.-E. Ting, J.-S. Lin *Nonlinear backstepping design of anti-lock braking system with assistance of active suspensions*, Proc. of the 16th IFAC World Congress, Prague, Jun 2005.